



Silica nanoparticle-based microfluidic immunosensor with laser-induced fluorescence detection for the quantification of immunoreactive trypsin



Marco A. Seia, Patricia W. Stege, Sirley V. Pereira, Irma E. De Vito, Julio Raba, Germán A. Messina*

INQUISAL, Department of Chemistry, National University of San Luis, CONICET, D5700BWS San Luis, Argentina

ARTICLE INFO

Article history:

Received 28 April 2014

Received in revised form 19 June 2014

Accepted 21 June 2014

Available online 28 June 2014

Keywords:

Newborn screening
Immunoreactive trypsin
Microfluidic chip
Silica nanoparticles
Ultrasonic procedure
LIF

ABSTRACT

The purpose of this study was to develop a silica nanoparticle-based immunosensor with laser-induced fluorescence (LIF) as a detection system. The proposed device was applied to quantify the immunoreactive trypsin (IRT) in cystic fibrosis (CF) newborn screening. A new ultrasonic procedure was used to extract the IRT from blood spot samples collected on filter papers. After extraction, the IRT reacted immunologically with anti-IRT monoclonal antibodies immobilized on a microfluidic glass chip modified with 3-aminopropyl functionalized silica nanoparticles (APSN-APTES-modified glass chips). The bounded IRT was quantified by horseradish peroxidase (HRP)-conjugated anti-IRT antibody (anti-IRT-Ab) using 10-acetyl-3,7-dihydroxyphenoxazine (ADHP) as enzymatic mediator. The HRP catalyzed the oxidation of nonfluorescent ADHP to highly fluorescent resorufin, which was measured by LIF detector, using excitation lambda at 561 nm and emission at 585 nm. The detection limits (LODs) calculated for LIF detection and for a commercial enzyme-linked immunosorbent assay (ELISA) test kit were 0.87 and 4.2 ng ml⁻¹, respectively. The within- and between-assay variation coefficients for the LIF detection procedure were below 6.5%. The blood spot samples collected on filter papers were analyzed with the proposed method, and the results were compared with those of the reference ELISA method, demonstrating a potential usefulness for the clinical assessment of IRT during the early neonatal period.

© 2014 Elsevier Inc. All rights reserved.

Nanomaterials are currently widely used for the construction of biosensors [1]. Among them, silica nanoparticles (SNs)¹ represent an interesting choice to be used in sensing [2–7] and as a support material [8–13] due to SNs' good monodispersity, high pore volume, and thermal and mechanical stability [14]. Furthermore, the large surface of SNs makes them an appropriate option for the immobilization of recognition biological moieties such as antibodies and antigens, allowing their use as solid support for immunoassays.

Quantitative immunological methods have been essential to many clinical, pharmaceutical, and scientific applications [15]. These methods can be performed in micrometer-scale analytical devices that consist of microchannels for transporting fluids with part or all of the necessary components of an integrated immuno-

assay [16–18]. The recent trend to miniaturize assays promotes the development of the microfluidic technology, which results in a substantial reduction in the consumption of reactive solutions [19], shorter analysis time, improved portability, and in part better detection limits (LODs) [20–23].

The use of nanoparticles as an immunological platform incorporated into a microfluidic device results in an increase in the effective area and the reduction of incubation times by reducing the diffusional distances [24].

Detection systems for microfluidic devices must be capable of providing sensitive measurements in low volumes. The most commonly used is laser-induced fluorescence (LIF) due to its high sensitivity and suitability for analyzing analytes in small volumes of fluid in chip formats [25].

The goal of this work was to develop a novel method to carry out cystic fibrosis (CF) newborn screening in a sensitive, fast, and automated way, measuring immunoreactive trypsin (IRT) in patients' blood. CF is an autosomal recessive disease and is also the most common severe genetic disease, found mainly in people of European descent with an incidence of approximately 1 in every 3000 live births worldwide [26–28,20]. The main characteristic of this pathology is the multi-organ involvement, including severe respiratory disease, pancreatic insufficiency, and male infertility

* Corresponding author. Fax: +54 2652 43 0224.

E-mail address: messina@unsl.edu.ar (G.A. Messina).

¹ Abbreviations used: SN, silica nanoparticle; LOD, detection limit; LIF, laser-induced fluorescence; CF, cystic fibrosis; IRT, immunoreactive trypsin; CCh, central channel; anti-IRT-Ab, anti-IRT antibody; HRP, horseradish peroxidase; ADHP, 10-acetyl-3,7-dihydroxyphenoxazine; PR, photoresist; HF, hydrofluoric acid; APTES, 3-aminopropyl triethoxysilane; ELISA, enzyme-linked immunosorbent assay; UV, ultraviolet; PDMS, poly(dimethylsiloxane); HPLC, high-performance liquid chromatography; APSN, 3-aminopropyl-functionalized silica nanoparticle; PBS, phosphate-buffered saline; RFU, relative fluorescence units; CV, coefficient of variation.

[21,29,23,30,31]. Depending on the country, the IRT cutoff value currently used for CF newborn screening ranges between 65 and 70 ng ml⁻¹ [32–34].

Because CF has no cure [35], an early and adequate diagnosis is essential.

To achieve the above-mentioned goal, SNs were incorporated into the central channel (CCh) of the microfluidic glass chip. The surface of SNs was functionalized with anti-IRT antibody (anti-IRT–Ab), which allowed the capture of IRT. The subsequent detection was achieved by adding horseradish peroxidase (HRP)-conjugated anti-IRT–Ab using 10-acetyl-3,7-dihydroxyphenoxazine (ADHP) as enzymatic mediator. The oxidation of ADHP to highly fluorescent resorufin was measured by LIF using excitation at 561 nm and emission at 585 nm.

The results indicated that our method, designed for the quantification of IRT, could provide a fast, sensitive, and automated CF diagnosis. Due to the benefits observed in the SN-based microfluidic immunosensor with LIF detection and the need for an early and adequate diagnosis, we believe that it could represent an attractive and alternative analytical strategy for CF newborn screening.

Materials and methods

Reagents and solutions

Soda lime glass wafers (26 × 76 × 1 mm) were purchased from Glass Técnica (São Paulo, Brazil). Sylgard 184 and AZ4330 photorealist (PR) were obtained from Dow Corning (Midland, MI, USA) and Clariant (Somerville, NJ, USA), respectively. Hydrofluoric acid (HF), 3-aminopropyl-functionalized silica (nanoparticles, ~100 nm particle size, DLS), 3-aminopropyl triethoxysilane (APTES), and ADHP were purchased from Sigma–Aldrich. Glutaraldehyde (25% aqueous solution) and acetone were purchased from Merck. The enzyme immunoassay for the quantitative determination of IRT, ImmunoChem Blood Spot Trypsin–MW ELISA (enzyme-linked immunosorbent assay) Kit (MP Biomedicals, USA), was purchased from Laboratorios Bacon (Argentina) and was used according to the manufacturer's instructions [36]. Anti-IRT–mouse monoclonal Ab (10 mg ml⁻¹) and HRP-conjugated anti-IRT–Ab (10 mg ml⁻¹) were purchased from Abcam (USA). All buffer solutions were prepared with Milli-Q water.

Instrumentation

The optical system was constructed using the procedure of Ref. [37] according to the following modification. A 532-nm single-frequency DPSS laser (Cobolt Jive, 561 nm, USA) operated at 25 mW served as the fluorescence excitation source. It was focused on the detection channel at 45° to the surface using a lens with a focal distance of 30 cm. The relative fluorescence signal of ADHP was measured using excitation at 561 nm and emission at 585 nm.

The paths of the reflected beams were arranged so that they did not strike the capillary channels elsewhere and to avoid photobleaching. The fluorescent radiation was detected with the optical axis of the assembly perpendicular to the plane of the device. Light was collected with a microscope objective (10:1, NA 0.30, working distance 6 mm, PZO, Poland) mounted on a microscope body (BIO-LAR L, PZO). A fiber-optic collection bundle was mounted on a sealed housing at the end of the lens of the microscope, which was connected to a QE65000-FL scientific-grade spectrometer (Ocean Optics, USA). The entire assembly was covered with a large box to eliminate ambient light.

The syringe pump system (Baby Bee Syringe Pump, Bioanalytical Systems) was used for pumping reagent solutions and stopping flow.

Absorbance was detected by a Bio-Rad Benchmark microplate reader (Japan) and a Beckman DU 520 general UV/VIS (ultraviolet/visible) spectrophotometer.

Microchip fabrication

The procedure for the fabrication of glass microfluidic chips is shown in Fig. 1. The construction was carried out according to the procedure described in Ref. [38] with the following modifications. The device layout was drawn using CorelDraw software version 11.0 (Corel) and printed on a high-resolution transparency film in a local graphic service, which was used as a mask in the photolithographic step. The microfluidic chip design consisted of a T-type format. The lengths of the central and accessory channels were 15 and 60 mm, respectively. The printed transparency mask was placed on top of a glass wafer previously coated with a 5- μ m layer of AZ4330 PR. The substrate was exposed to UV radiation for 30 s and developed in AZ 400 K developer solution for 2 min. Glass channels were etched with an etching solution of 20% HF for 4 min under continuous stirring (check the HF material safety data sheet). The etching rate was $8 \pm 1 \mu\text{m min}^{-1}$. Following the etching step, substrates were rinsed with deionized water and the PR was removed with acetone. To access the microfluidic network, holes were drilled on glass-etched channels with a Dremel tool (MultiPro 395JU model, USA) using 1-mm diamond drill bits.

To achieve the final chip format, another glass plate was spin-coated with a thin poly(dimethylsiloxane) (PDMS) layer at 3000 rpm for 10 s. PDMS was prepared with a 10:1 mixture of Sylgard 184 elastomer and a curing agent. The thickness of this layer was 50 μ m. Before sealing, the PDMS layer was cured at 100 °C for 5 min on a hot plate. Glass channels and PDMS-coated glass substrate were placed in an oxygen plasma cleaner (Plasma Technology PLAB SE80 plasma cleaner) and oxidized for 1 min. The two pieces were brought into contact immediately after the plasma treatment, obtaining a strong and irreversible sealing. The final device format was achieved in less than 30 min. The bonding resistance of the device was evaluated under different pressure values by using a high-performance liquid chromatography (HPLC) pump. The flow rate ranged from 10 to 300 $\mu\text{l min}^{-1}$.

Glass chip surface modification

Coating of central channel's chip with APTES

The CCh was pretreated according to the following steps: washed for 15 min with 1 M HCL, rinsed for 15 min with deionized water, and rinsed for 15 min with methanol at 2 $\mu\text{l min}^{-1}$. After the preconditioning procedure, the 2.5% (v/v) APTES in methanol solution was introduced into the glass channel inner surface at 2 $\mu\text{l min}^{-1}$ for 30 min. It was left to stand filled with the silanization solution for 2 h (Fig. 2). Then, the channel was rinsed with methanol and dried under a nitrogen flow.

Immobilization of APSNs onto APTES-modified glass chip surface

We mixed 1 mg of 3-aminopropyl-functionalized silica nanoparticles (APSNs) with 1 ml of aqueous solution of 5% (w/w) glutaraldehyde in 0.20 M CO₃²⁻/HCO₃⁻ buffer (pH 10.0) to induce the formation of aldehyde groups at 25 °C for 2 h. Then, glutaraldehyde–APSNs were pumped into the CCh of APTES-modified glass chip at 2 $\mu\text{l min}^{-1}$ for 10 min. After that, it was left to stand filled with the same solution for 60 min and finally rinsed with phosphate buffer (pH 7.2) for 15 min (Fig. 2).

Covalent binding of IRT-specific Ab onto APSN–APTES-modified glass chip surface

A solution of 10 $\mu\text{g ml}^{-1}$ anti-IRT–Ab in 0.10 M phosphate buffer (pH 7.2) was injected through the CCh of the modified chip and

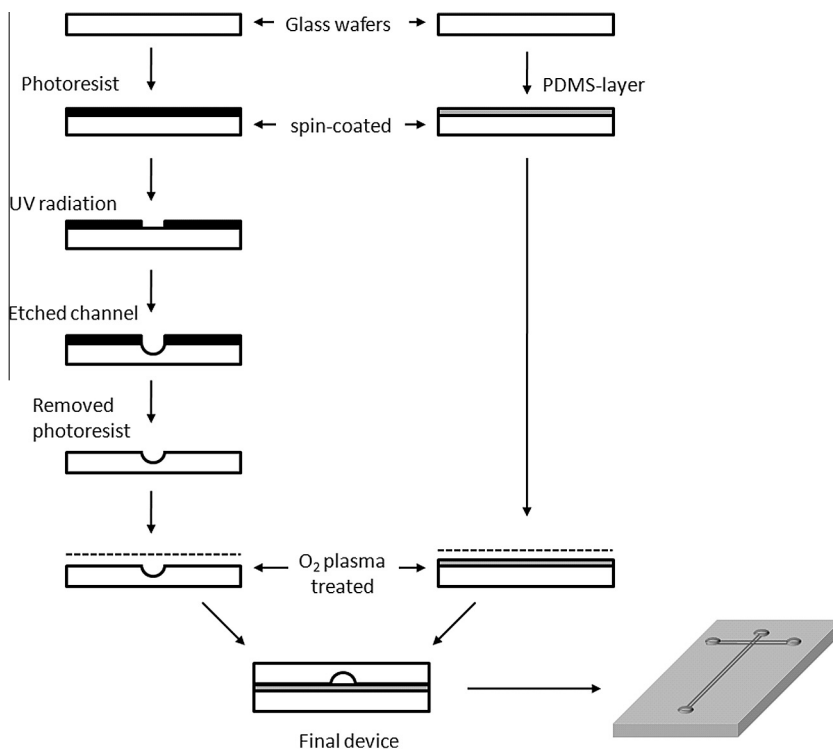


Fig. 1. Microfabrication process of glass microfluidic chip with sealing procedure based on the use of a thin layer of PDMS. The process involves wet chemical etching of glass with 20% HF for 4 min under continuous stirring, spin-coating of a PDMS and photoresist layer over flat glass surface at 3000 rpm for 15 s, and plasma-oxidized treatment for 1 min.

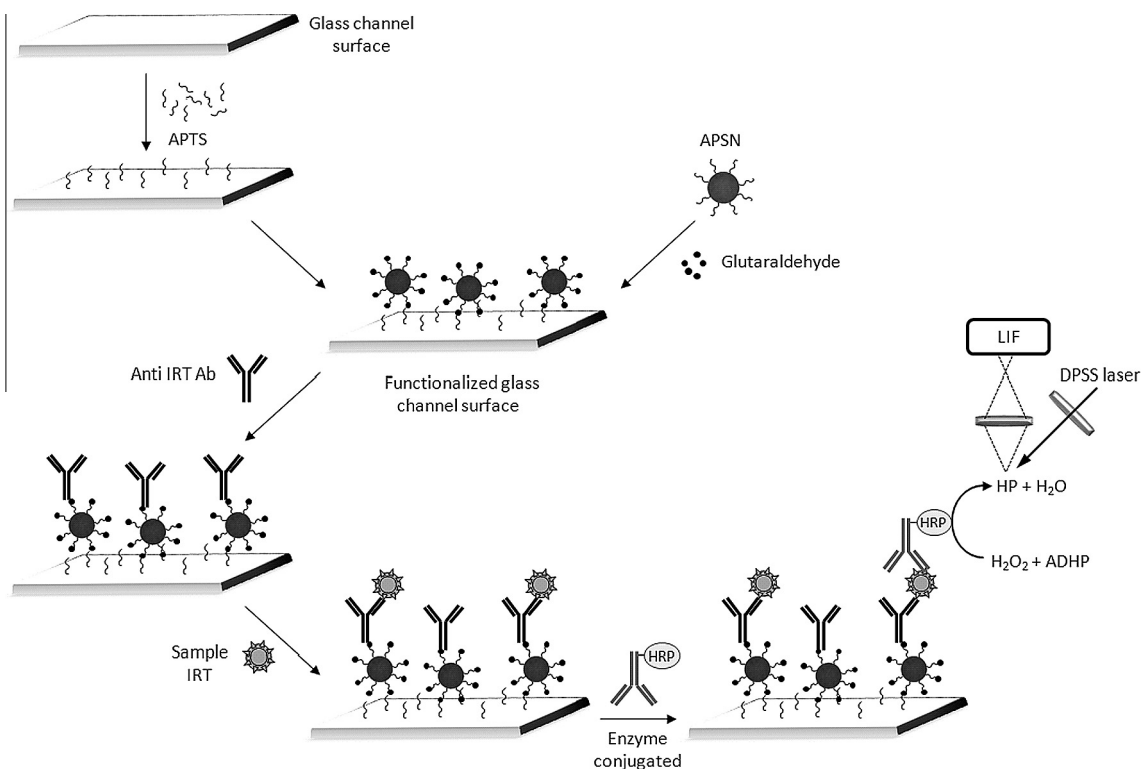


Fig. 2. Schematic representation of the glass chip surface modification and the immunological reaction. Anti-IRT-Ab were covalently bound onto APSNs that were covalently attached over APTES-modified glass chip surface. The IRT present in the blood spot collected filter papers reacted immunologically with anti-IRT-Ab-immobilized APSNs-APTES-modified glass chips. The bound IRT was quantified by HRP-conjugated anti-IRT-Ab using ADHP as enzymatic mediator. The highly fluorescent resorufin (HP) generated was measured by LIF using excitation at 561 nm and emission at 585 nm.

left to react at 25 °C for 2 h (Fig. 2). Finally, the CCh was rinsed with phosphate buffer (pH 7.2) to remove the unbound anti-IRT-Ab and stored in the same buffer at 4 °C. Residual aldehyde groups of glutaraldehyde present on the APSN surface allowed the covalent attachment of the amino groups of anti-IRT-Ab (Fig. 2). The antibody preparation was left stable for at least 1 month.

Preparation of sample

For the quantification of human IRT, blood samples were spotted in filter paper number 903 in the center of a 1-cm circle and allowed to diffuse outward, trying to avoid tearing or disrupting the filter paper surface. The specimens were allowed to air dry completely (overnight), avoiding heat, direct sunlight, and absorbent surfaces. After drying overnight, these were stored in an airtight plastic envelope at less than –15 °C until assay. In this work, we used neonatal samples and control samples provided by the Blood Spot Trypsin-MW ELISA Kit.

To start the IRT measurement, a disk was punched from a blood spot collected filter paper number 903. After that, it was placed into an Eppendorf tube with 200 μl in 0.01 M phosphate-buffered saline (PBS, pH 7.2) and exposed to a sonication procedure for 2 min. To compare IRT extraction procedures, our proposed ultrasonic extraction process and the Blood Spot Trypsin-MW ELISA Kit were performed simultaneously. In both cases, the content of all tubes was aspirated and the eluted samples were stored at 4 °C until use.

IRT LIF determination

The IRT determination process included several steps in which reactive and washing solutions were pumped at a flow rate of 2.0 $\mu\text{l min}^{-1}$. After each reagent solution injection, the CCh of the device was exposed to a washing procedure with 0.01 M PBS (pH 7.2) for 5 min in order to remove the reagent excess.

As a first step, a blocking treatment was performed through injecting 1% of bovine serum albumin (BSA) in 0.01 M PBS (pH 7.2) for 5 min in order to avoid unspecific bindings. Once the device was blocked, the eluted sample was injected into the PBS carrier stream for 10 min. The Ab bounded on the APSNs in the CCh wall reacted with IRT present in the eluted sample. Bound IRT was quantified using HRP-conjugated anti-IRT-Ab (dilution of 1:1000 in 0.01 M PBS, pH 7.2) injected for 5 min.

For the relative fluorescence measurement, the substrate solution was prepared by dissolving 0.01 M ADHP stock solution in dimethyl sulfoxide (DMSO) and stored at –20 °C. The ADHP solution previously obtained and the H_2O_2 solution were diluted to 0.001 M with 0.1 M phosphate-citrate buffer (pH 5.05) before being used. The substrate solution was injected into the carrier stream for 1 min, and the enzymatic product was measured by LIF. The HRP in the presence of H_2O_2 catalyzed the oxidation of nonfluorescent ADHP to highly fluorescent resorufin, which was measured using excitation at 561 nm and emission at 585 nm.

After each sample measurement, the device was exposed to a flow of desorption buffer (0.1 M glycine-HCl, pH 2.0) at a flow rate of 2.0 $\mu\text{l min}^{-1}$ for 5 min and then washed with PBS (pH 7.2). With this treatment, bound immunocomplexes were desorbed, allowing us to start with the next determination. The storage of the device was done in 0.01 M PBS (pH 7.2) at 4 °C. The proposed device could be used with no significant loss of sensitivity for 15 days, whereas its useful lifetime was 1 month with a sensitivity decrease of 10%. The storage of the device was done in 0.01 M PBS (pH 7.2) at 4 °C. Table A in the online [supplementary material](#) summarizes the complete analytical procedure required for the IRT immunoassay.

Results and discussion

Optimization

APSN-APTES amplification effect

To evaluate the signal amplification effect of silica nanoparticles, we compared the signal intensity of APSN-APTES-modified glass chips with the signal obtained from the microfluidic glass chip modified only with APTES over the flat CCh surface using HRP as an indicator model. For these experiments, on the one hand, the CCh was modified according to the procedure explained in the first and second subsections of the “Glass chip surface modification” section in Materials and Methods. On the other hand, the microfluidic glass chip was modified only with APTES according to the procedure explained in the first subsection. After that, a solution of 10 $\mu\text{g ml}^{-1}$ HRP in 0.10 M phosphate buffer (pH 7.2) was injected through the CCh of both chips and left to react at 25 °C for 2 h. Finally, the CCh was rinsed with phosphate buffer (pH 7.2) to remove the unbound HRP and stored in the same buffer at 4 °C. The HRP toward the reduction of H_2O_2 catalyzed the oxidation of nonfluorescent ADHP to highly fluorescent resorufin, which was measured by LIF, using excitation at 561 nm and emission at 585 nm. According to the obtained results, APSN incorporated into the channel generated important signal amplification, more than 4 times compared with the flat channel surface (Fig. 3).

Effects of flow rate and incubation times

The flow rates of samples and reagents have a significant effect on the efficiency of antigen-antibody interactions in microfluidic immunosensors. This effect is based on the fact that in microfluidic devices, unlike conventional immunoassays, samples and reagents are continuously flowing through the device.

For the determination of IRT, the flow rate was analyzed by studying the relative fluorescence obtained in the IRT control sample of 154 ng ml^{-1} at different flow rates: 1, 2, 3, 4, 5, and 6 $\mu\text{l min}^{-1}$ (Fig. 4). The response signal was significantly reduced when the flow rate exceeded 3 $\mu\text{l min}^{-1}$. Therefore, a flow rate of 2 $\mu\text{l min}^{-1}$ was used for samples, reagents, and washing solutions.

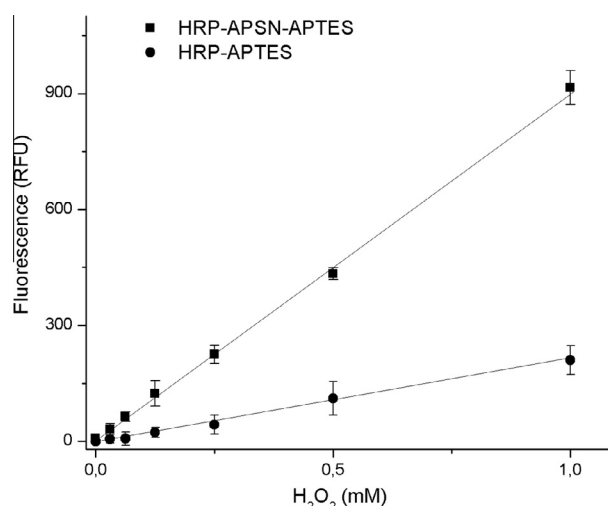


Fig. 3. Evaluation of signal amplification effect of APSNs. A comparison between the signal intensity of the proposed method (APSN-APTES-modified glass chip) with the signal obtained from the microfluidic glass chip modified only with APTES over the flat CCh surface using HRP as an indicator model was carried out. For this study, 0.1 M phosphate-citrate buffer (pH 5.05) containing different concentrations of H_2O_2 and 0.001 M ADHP was injected into the carrier stream at a flow rate of 2 $\mu\text{l min}^{-1}$, and the enzymatic product was measured by LIF using an excitation wavelength of 561 nm and an emission wavelength of 580 nm. RFU, relative fluorescence units.

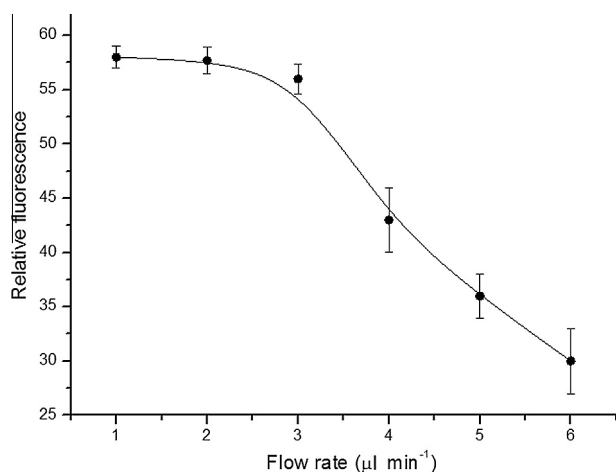


Fig. 4. Effect of flow rate analyzing a 154-ng ml⁻¹ IRT control sample at different flow rates. Here, 0.1 M phosphate-citrate buffer (pH 5.05) containing 0.001 M H₂O₂ and 0.001 M ADHP was injected into the carrier stream at different flow rates. The enzymatic product was measured by LIF using an excitation wavelength of 561 nm and an emission wavelength of 580 nm.

Regarding incubation time, the minimum time required for IRT binding is also a critical assay factor, especially when the use of a minimum total analysis time is desired. Fig. 5 shows the measured fluorescence for 53, 154, 282, and 580 ng ml⁻¹ IRT control sample concentrations. The fluorescence intensity increased when the IRT concentration grew. As expected, the intensity of the fluorescence increased with the reaction time. The intensity of the fluorescence, however, did not increase considerably until 10 min had passed, which was likely due to saturation of the specific antibody sites in the APSN-APTES-modified glass chips. Therefore, the optimal reaction time was 10 min.

A study of the rates of enzymatic response under flow conditions was performed in the pH range of 3.0 to 8.0 and showed a maximum value of activity at pH 5.05 (data not shown). Besides, the enzyme exhibits its best activity over the temperature range of 20 to 25 °C; higher temperatures would be harmful to its activity [39].

Ultrasonic procedure for IRT extraction

We compared our ultrasonic procedure for the IRT extraction and the Trypsin-MW ELISA Kit procedure as has already been explained. For this experiment, two high-level control samples, two high-level neonatal samples, two low-level control samples, and two low-level neonatal samples were compared using both extraction procedures for the IRT blood spot elution. After that, all of these samples were analyzed by our LIF immunosensor and

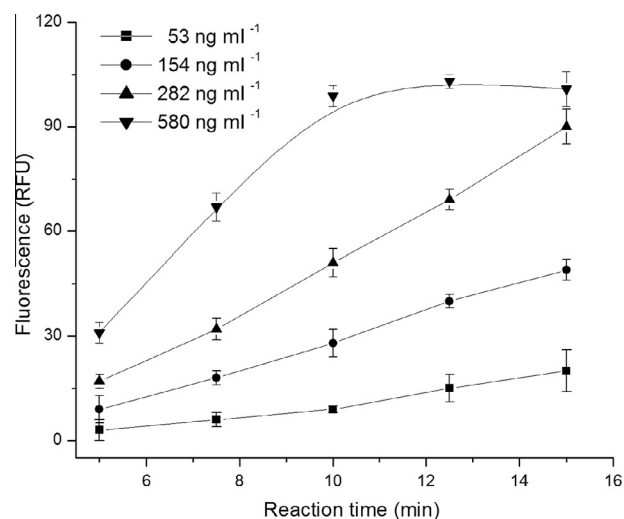


Fig. 5. Fluorescence intensity as a function of reaction time for 53, 154, and 580 ng ml⁻¹ of IRT control sample concentrations. The flow rate was 2 µl min⁻¹. Here, 0.1 M phosphate-citrate buffer (pH 5.05) containing 0.001 M H₂O₂ and 0.001 M ADHP was injected into the carrier stream at different flow rates. The enzymatic product was measured by LIF using an excitation wavelength of 561 nm and an emission wavelength of 580 nm.

Blood Spot Trypsin-MW ELISA Kit. As shown in Table 1, we obtained similar IRT concentrations employing both procedures for all neonatal samples and control samples analyzed, indicating a good correspondence between them. The acquired results prove that APSN-APTES-modified glass chips have excellent selectivity and sensitivity for the specific detection of IRT antigens.

Quantitative test for detection of IRT in APSN-APTES-modified glass chips

The IRT calibration plot was obtained by plotting relative fluorescence versus IRT concentration in the range of 0 to 580 ng ml⁻¹. A linear relation, relative fluorescence units (RFU) = 0.281 + 0.179 × C_{IRT}, was obtained. The correlation coefficient (*r*) for this plot was 0.998. The coefficient of variation (CV) for determination of the IRT control sample of 154 ng ml⁻¹ was below 5% (six replicates). The LOD is the concentration that gives a signal 3 times the standard deviation of the blank. For LIF detection procedures and the ELISA test kit, the LODs were 0.87 and 4.20 ng ml⁻¹, respectively. This indicates that the proposed method exhibits a wide measurable concentration range and a low LOD.

The precision of the proposed method was checked with IRT control samples at 53-, 154-, and 580-ng ml⁻¹ concentrations. This

Table 1

Comparison between ultrasonic and Trypsin-MW ELISA Kit procedures for the IRT blood spot extraction, analyzed by the proposed method and the Trypsin-MW ELISA Kit (five measurements in the same run for each control sample).

Sample number (IRT ng ml ⁻¹)	IRT Ultrasonic procedure extraction		^a IRT ELISA Kit procedure extraction	
	Immunosensor (IRT ng ml ⁻¹)	ELISA kit ^a (IRT ng ml ⁻¹)	Immunosensor (IRT ng ml ⁻¹)	ELISA kit ^a (IRT ng ml ⁻¹)
HLCS ₁	96.3 ± 3.3	97.9 ± 5.2	96.6 ± 2.6	96.4 ± 4.6
HLCS ₂	223.2 ± 8.4	226.7 ± 7.5	222.9 ± 9.1	219.8 ± 8.7
HLNS ₁	310.3 ± 12.2	317.9 ± 16.8	313.4 ± 11.9	311.3 ± 13.9
HLNS ₂	256.5 ± 10.7	252.4 ± 8.9	253.7 ± 9.5	259.2 ± 11.3
LLCS ₁	54.3 ± 1.4	56.4 ± 2.2	55.4 ± 2.6	55.3 ± 2.9
LLCS ₂	26.2 ± 0.8	26.8 ± 1.2	27.3 ± 1.1	26.8 ± 1.6
LLNS ₁	33.4 ± 1.2	32.9 ± 1.8	32.6 ± 1.1	31.7 ± 1.3
LLNS ₂	22.1 ± 0.7	22.4 ± 0.9	22.7 ± 0.4	21.9 ± 1.0

Note. HLCS, high-level control samples; HLNS, high-level neonatal samples; LLCS, low-level control samples; LLNS, low-level neonatal samples.

^a Trypsin-MW ELISA Kit.

Table 2

Within-assay precision (five measurements in the same run for each IRT control sample) and between-assay precision (five measurements for each IRT control sample, repeated for 3 consecutive days).

Control sample ^a (ng ml ⁻¹)	Within assay		Between assay	
	Mean	CV%	Mean	CV%
53	52.64	4.26	52.13	4.81
154	154.72	4.94	157.53	6.42
580	581.77	2.59	586.82	5.26

^a ng ml⁻¹ IRT control sample.

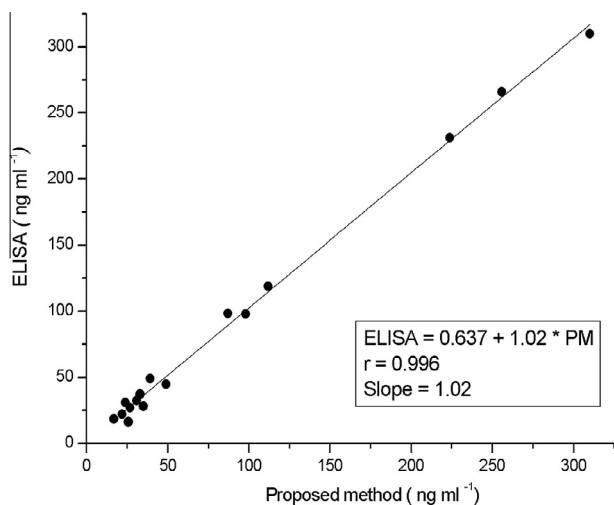


Fig. 6. Correlation between proposed method and ELISA. PM, proposed method.

series of analyses was repeated for 3 consecutive days in order to estimate the between-assay precision. The IRT assay showed CV within-assay values that were below 5%, and the CV between-assay values were below 6.5% (Table 2).

The accuracy of the LIF immunosensor was tested with a dilution test performed using an IRT control sample of 580 ng ml⁻¹ that was serially diluted in 0.01 M PBS (pH 7.2). The linear regression equation was RFU = 0.491 + 107.01 × C_{IRT}, with a linear regression coefficient $r = 0.997$ (see supplementary material).

In addition, the proposed method was compared with a commercial ELISA procedure for the quantification of IRT in neonatal samples. The slopes obtained were reasonably close to 1, indicating a good correspondence between the two methods (Fig. 6).

In this work, we analyzed three IRT high-level neonatal samples, three IRT high-level control samples (provided with the Trypsin-MW ELISA Kit), and 10 low-level neonatal samples. All samples had been previously confirmed for IRT levels using the commercial Trypsin-MW ELISA Kit. High-level samples and controls were later analyzed by our proposed quantitative method, which revealed high concentrations of IRT in all of them. The analysis of the low-level samples also showed low concentrations of IRT.

The total assay time required for the determination of IRT concentration using the proposed method was 37 min without the ultrasonic sample elution preparation and less than 40 min including it. The conventional batch-well ELISA employs an assay time of 2 h without the sample elution procedure and approximately 10 h including the sample elution procedure provided by the Blood Spot Trypsin-MW ELISA Kit.

According to an intensive search, few previously reported articles were found on IRT detection. First, Xu and coworkers proposed an assay based on immunoreagents labeled with lanthanide ions, on dissociative fluorescence enhancement applying the principle

of cofluorescence, and on time-resolved fluorometry [40]. Second, Lindau-Shepard and Pass developed a multiplex immunoassay using two different Luminex bead sets for IRT isoform detection [41]. It is relevant to emphasize that the proposed method is based on microfluidic technology, coupled to LIF detection, with an APSN-APTES biorecognition platform that allowed the successful immobilization of anti-IRT-Ab as a strategy to provide specificity to the device. In addition, the achieved LOD was lower than that obtained by the above-mentioned articles [40,41]. Considering the CF neonatal screening cutoff value, all obtained LODs were reasonably good. Thus, we came to the conclusion that our device has inherent benefits such as miniaturization, integration, portability, and the possibility to perform on-site analysis.

Conclusions

In this research, we successfully performed the microfabrication of a glass microfluidic chip sealed by a thin layer of PDMS together with the modification of the glass channel surface by anti-IRT-Ab covalently bounded onto APSN-APTES-modified glass chip. This modified microfluidic chip was applied to the CF newborn screening through the selective and sensitive quantification of IRT in neonatal blood samples. In addition, we proposed and evaluated a new ultrasonic procedure for the IRT blood spot extraction collected on filter papers. This allowed us to obtain an important reduction of the elution time compared with the extraction process proposed by the conventional ELISA analysis. The total assay time for IRT determination by the proposed method was less than 40 min considering the sample elution step, whereas the conventional batch-well ELISA requires approximately 10 h of time consumption including the sample elution step. Our developed system combines the high sensitivity of LIF detection and the inherent properties of optical fibers (e.g., chemical inertness of the surface, high transmission, flexibility, low cost) with microfluidic technology features, which translates into more rapid manipulation, lower power requirements, and increased portability of the device. To conclude, the APSN-APTES-modified glass chip described above enables a fast, accurate, and selective IRT analysis during the early neonatal period, demonstrating its potential usefulness for CF newborn screening.

Acknowledgments

The authors are thankful for financial support from the Universidad Nacional de San Luis, the Agencia Nacional de Promoción Científica y Tecnológica, and the Consejo Nacional de Investigaciones Científicas y Técnicas (CONICET).

Appendix A. Supplementary data

Supplementary data associated with this article can be found, in the online version, at <http://dx.doi.org/10.1016/j.ab.2014.06.016>.

References

- [1] T. Asefa, C.T. Duncan, K.K. Sharma, Recent advances in nanostructured chemosensors and biosensors, *Analyst* 134 (2009) 1980–1990.
- [2] Q. Wei, R. Li, B. Du, D. Wu, Y.Y. Han, Y.Y. Cai, Y.F. Zhao, X.D. Xin, H. Li, M.H. Yang, Multifunctional mesoporous silica nanoparticles as sensitive labels for immunoassay of human chorionic gonadotropin, *Sens. Actuators, B* 153 (2011) 256–260.
- [3] Q. Wei, X.D. Xin, B. Du, D. Wu, Y.Y. Han, Y.F. Zhao, Y.Y. Cai, R. Li, M.H. Yang, H. Li, Electrochemical immunosensor for norethisterone based on signal amplification strategy of graphene sheets and multienzyme functionalized mesoporous silica nanoparticles, *Biosens. Bioelectron.* 26 (2010) 723–729.
- [4] D. Wu, R. Li, H.X. Wang, S.Q. Liu, H. Wang, Q. Wei, B. Du, Hollow mesoporous silica microspheres as sensitive labels for immunoassay of prostate-specific antigen, *Analyst* 137 (2012) 608–613.

- [5] J.H. Lin, Z.J. Wei, C.M. Mao, A label-free immunosensor based on modified mesoporous silica for simultaneous determination of tumor markers, *Biosens. Bioelectron.* 29 (2011) 40–45.
- [6] Y.Y. Cai, H. Li, B. Du, M.H. Yang, Y. Li, D. Wu, Y.F. Zhao, Y.X. Dai, Q. Wei, Ultrasensitive electrochemical immunoassay for BRCA1 using BMIM-BF₄-coated SBA-15 as labels and functionalized graphene as enhancer, *Biomaterials* 32 (2011) 2117–2123.
- [7] Y. Wu, C. Chen, S. Liu, Enzyme-functionalized silica nanoparticles as sensitive labels in biosensing, *Anal. Chem.* 81 (2009) 1600–1607.
- [8] H. Wang, Y. Zhang, H.Q. Yu, D. Wu, H.M. Ma, H. Li, B. Du, Q. Wei, Label-free electrochemical immunosensor for prostate-specific antigen based on silver hybridized mesoporous silica nanoparticles, *Anal. Biochem.* 434 (2013) 123–127.
- [9] S. Liu, Q. Lin, X.M. Zhang, X.R. He, X.R. Xing, W.J. Lian, J. Li, M. Cui, J.D. Huang, Electrochemical immunosensor based on mesoporous nanocomposites and HRP-functionalized nanoparticles bioconjugates for sensitivity enhanced detection of diethylstilbestrol, *Sens. Actuators, B* 562 (2012) 166–167.
- [10] J.H. Lin, Z.J. Wei, H.H. Zhang, M.J. Shao, Sensitive immunosensor for the label-free determination of tumor marker based on carbon nanotubes/mesoporous silica and graphene modified electrode, *Biosens. Bioelectron.* 41 (2013) 342–347.
- [11] B.Q. Liu, B. Zhang, Y.L. Cui, H.F. Chen, Z.Q. Gao, D.P. Tang, Multifunctional gold-silica nanostructures for ultrasensitive electrochemical immunoassay of streptomycin residues, *ACS Appl. Mater. Interfaces* 3 (2011) 4668–4676.
- [12] D. Tang, B. Su, J. Tang, J. Ren, G. Chen, Nanoparticle-based sandwich electrochemical immunoassay for carbohydrate antigen 125 with signal enhancement using enzyme-coated nanometer-sized enzyme-doped silica beads, *Anal. Chem.* 82 (2010) 1527–1534.
- [13] J. Wang, G. Liu, M.H. Engelhard, Y. Lin, Sensitive immunoassay of a biomarker tumor necrosis factor- α based on poly(guanine)-functionalized silica nanoparticle label, *Anal. Chem.* 78 (2006) 6974–6979.
- [14] L.L. Chen, Z.J. Zhang, P. Zhang, X.M. Zhang, A.H. Fu, An ultra-sensitive chemiluminescence immunosensor of carcinoembryonic antigen using HRP-functionalized mesoporous silica nanoparticles as labels, *Sens. Actuators, B* 155 (2011) 557–561.
- [15] C.H. Self, D.B. Cook, Advances in immunoassay technology, *Curr. Opin. Biotechnol.* 7 (1996) 60–65.
- [16] H. Becker, L.E. Locascio, Polymer microfluidic devices, *Talanta* 56 (2002) 267–287.
- [17] S.K. Sia, G.M. Whitesides, Microfluidic devices fabricated in poly(dimethylsiloxane) for biological studies, *Electrophoresis* 24 (2003) 3563–3576.
- [18] D. Erickson, D. Li, Integrated microfluidic devices, *Anal. Chim. Acta* 507 (2004) 11–26.
- [19] J. Wang, Portable electrochemical systems, *Trends Anal. Chem.* 21 (2002) 226–232.
- [20] C. Farra, R. Menassa, J. Awwad, Y. Morel, P. Salameh, N. Yazbeck, M. Majdalani, R. Wakim, K. Yunis, S. Mroueh, F. Cabet, Mutational spectrum of cystic fibrosis in the Lebanese population, *J. Cyst. Fibros.* 9 (2010) 406–410.
- [21] C. Colombo, P.M. Battezzati, A. Crosignani, A. Morabito, D. Costantini, R. Padoan, A. Giunta, Liver disease in cystic fibrosis: a prospective study on incidence, risk factors, and outcome, *Hepatology* 36 (2002) 1374–1382.
- [22] M.R. Knowles, P.R. Durie, What is cystic fibrosis?, *N Engl. J. Med.* 347 (2002) 439–442.
- [23] A. Lindblad, H. Glaumann, B. Strandvik, Natural history of liver disease in cystic fibrosis, *Hepatology* 30 (1999) 1151–1158.
- [24] J.W. Choi, K.W. Oh, J.H. Thomas, W.R. Heineman, H.B. Halsall, J.H. Nevin, A.J. Helmicki, H.T. Henderson, C.H. Ahn, An integrated microfluidic biochemical detection system for protein analysis with magnetic bead-based sampling capabilities, *Lab Chip* 2 (2002) 27–30.
- [25] M.E. Johnson, J.P. Landers, Fundamentals and practice for ultrasensitive laser-induced fluorescence detection in microanalytical systems, *Electrophoresis* 25 (2004) 3513–3527.
- [26] H. Corvol, J. Beucher, P. Boëlle, P. Busson, C. Muselet-Charlier, A. Clement, F. Ratjen, H. Grasemann, J. Laki, C.N.A. Palmer, J.S. Elborn, A. Mehta, Ancestral haplotype 8.1 and lung disease severity in European cystic fibrosis patients, *J. Cyst. Fibros.* 11 (2012) 63–67.
- [27] D. Debray, D. Kelly, R. Houwen, B. Strandvik, C. Colombo, Best practice guidance for the diagnosis and management of cystic fibrosis-associated liver disease, *J. Cyst. Fibros.* 10 (2011) 29–36.
- [28] A. Leonard, P. Lebecque, J. Dingemans, T. Leal, A randomized placebo-controlled trial of miglustat in cystic fibrosis based on nasal potential difference, *J. Cyst. Fibros.* 11 (2012) 231–236.
- [29] M.R. Knowles, P.R. Durie, In vivo nasal potential difference: techniques and protocols for assessing efficacy of gene transfer in cystic fibrosis, *N. Engl. J. Med.* 347 (2002) 439–442.
- [30] B.J. Rosenstein, G.R. Cutting, The diagnosis of cystic fibrosis: a consensus statement, *J. Pediatr.* 132 (1998) 589–595.
- [31] C.E. Wainwright, A.L. Quittner, D.E. Geller, C. Nakamura, J.L. Wooldridge, R.L. Gibson, S. Lewis, A.B. Montgomery, Aztreonam for inhalation solution (AZLI) in patients with cystic fibrosis, mild lung impairment, and *P. aeruginosa*, *J. Cyst. Fibros.* 10 (2011) 234–242.
- [32] R. Weber, M. Pavan, A. Canto de Souza, S. Martins de Castro, An evaluation of IRT neonatal analytical performance in AutoDELTA, *J. Bras. Patol. Med. Lab.* 49 (2013) 388–390.
- [33] O. Sommerburg, V. Krulisova, J. Hammermann, M. Lindner, N.M. Stahl, M. Muckenthaler, D. Kohlmueller, M. Happich, A.E. Kulozik, F. Votava, M. Balascakova, V. Skalicka, M. Stopsack, M. Gahr, M. Macek Jr., M.A. Mall, G.F. Hoffmann, Comparison of different IRT-PAP protocols to screen newborns for cystic fibrosis in three central European populations, *J. Cyst. Fibros.* 13 (2014) 15–23.
- [34] J. Sarles, R. Giorgi, P. Berthézène, A. Munck, D. Cheillan, J.C. Dagorn, M. Roussey, Neonatal screening for cystic fibrosis: comparing the performances of IRT/DNA and IRT/PAP, *J. Cyst. Fibros.* 13 (2014) 384–390.
- [35] C. Minasian, A. McCullagh, A. Bush, Cystic fibrosis in neonates and infants, *Early Hum. Dev.* 81 (2005) 997–1004.
- [36] MP Biomedicals, ImmunoChem Blood Spot Trypsin-MW ELISA Kit, MP Biomedicals, 2011.
- [37] K. Seiler, D.J. Harrison, A. Manz, Planar glass chips for capillary electrophoresis: repetitive sample injection, quantitation, and separation efficiency, *Anal. Chem.* 65 (1993) 1481–1488.
- [38] T.P. Segato, W.K. Coltro, A.L. Almeida, M.H. Piazetta, A.L. Gobbi, L.H. Mazo, E. Carrilho, A rapid and reliable bonding process for microchip electrophoresis fabricated in glass substrates, *Electrophoresis* 31 (2010) 2526–2533.
- [39] G.D. Liu, J.T. Yan, G.L. Shen, R.Q. Yu, Renewable amperometric immunosensor for complement 3 (C₃) assay in human serum, *Sens. Actuators, B* 80 (2001) 95–100.
- [40] Y.Y. Xu, K. Pettersson, K. Blomberg, I. Hemmilä, H. Mikola, T. Lövgren, Simultaneous quadruple-label fluorometric immunoassay of thyroid-stimulating hormone, 17 α -hydroxyprogesterone, immunoreactive trypsin, and creatine kinase MM isoenzyme in dried blood spots, *Clin. Chem.* 38 (1992) 2038–2043.
- [41] B.A. Lindau-Shepard, K.A. Pass, Newborn screening for cystic fibrosis by use of a multiplex immunoassay, *Clin. Chem.* 56 (2010) 445–450.